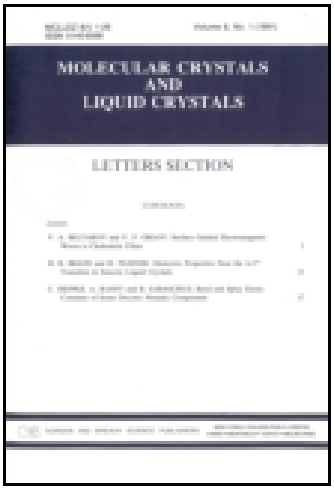

Molecular Crystals and Liquid Crystals
Publication details, including instructions for authors and subscription information:
http://www.tandfonline.com/loi/gmcl20

Simulating Quantum-Mechanical Barrier Tunneling Phenomena with a Nematic-Liquid-Crystal-Filled Double-Prism Structure

Andreas C. Liapis[a], George M. Gehring[a], Svetlana G. Lukishova[a] & Robert W. Boyd[ab]

[a] The Institute of Optics, University of Rochester, Rochester, NY, USA

[b] Department of Physics and School of Electrical Engineering and Computer Science, University of Ottawa, Ottawa, ON, Canada

Published online: 30 Sep 2014.

To cite this article: Andreas C. Liapis, George M. Gehring, Svetlana G. Lukishova & Robert W. Boyd (2014) Simulating Quantum-Mechanical Barrier Tunneling Phenomena with a Nematic-Liquid-Crystal-Filled Double-Prism Structure, Molecular Crystals and Liquid Crystals, 595:1, 136-143, DOI: 10.1080/15421406.2014.918084

To link to this article: http://dx.doi.org/10.1080/15421406.2014.918084

Mol. Cryst. Liq. Cryst., Vol. 595: pp. 136–143, 2014

ISSN: 1542-1406 print/1563-5287 online
DOI: 10.1080/15421406.2014.918084

Taylor & Francis
Taylor & Francis Group

Simulating Quantum-Mechanical Barrier Tunneling Phenomena with a Nematic-Liquid-Crystal-Filled Double-Prism Structure

ANDREAS C. LIAPIS,[1,*] GEORGE M. GEHRING,[1] SVETLANA G. LUKISHOVA,[1] AND ROBERT W. BOYD[1,2]

[1]The Institute of Optics, University of Rochester, Rochester, NY, USA
[2]Department of Physics and School of Electrical Engineering and Computer Science, University of Ottawa, Ottawa, ON, Canada

We present an electrically-controlled nematic-liquid-crystal-filled double-prism structure that can be used to simulate quantum-mechanical tunneling through a barrier of variable height. Measurements of time delay in reflection from this structure, taken with femtosecond resolution using entangled photon pairs in a Hong-Ou-Mandel interferometer, are compared to theoretical predictions. We show that the Goos-Hänchen contribution to the tunneling delay is unmeasurable in this geometry. Our research contributes to the understanding of quantum-mechanical barrier tunneling times, and can lead to the fabrication of optical analogues to the tunnel junction and other photonic devices.

Keywords Liquid crystals; pulse propagation; tunneling; Goos-Hänchen shift

1. Introduction

The process of quantum mechanical barrier tunneling, whereby a particle of energy E encounters a finite potential barrier of height $V_0 > E$, has been a topic of intense scrutiny for the better part of a century. Whereas the determination of the transmission and reflection probabilities is a fairly straightforward exercise in undergraduate quantum mechanics, the time delay experienced by the particle has been the cause of much controversy. The traditional definition of the group delay τ_g acquired when tunneling through a barrier of length L is calculated by the method of stationary phase, and is frequently called the phase time or Wigner time [1]. Surprisingly, the group delay can, under certain conditions, become shorter than the "equal time" c/L, suggesting superluminal transit of the tunneled particle. Many attempts have been made to resolve this apparent paradox [2], and the ongoing debate has made it evident that further experimental investigations of these effects are required.

It is commonly accepted that time delays in frustrated total internal reflection (FTIR) form an optical analog to these quantum-mechanical tunneling times [3–5]. Indeed, the evanescent waves supported by such a structure decay in a manner reminiscent of quantum mechanical wave functions in a potential barrier (Fig. 1). Studying optical time delays in such structures can help us shed light on these paradoxical tunneling phenomena. However,

*Address correspondence to Andreas C. Liapis; E-mail: liapis@optics.rochester.edu.

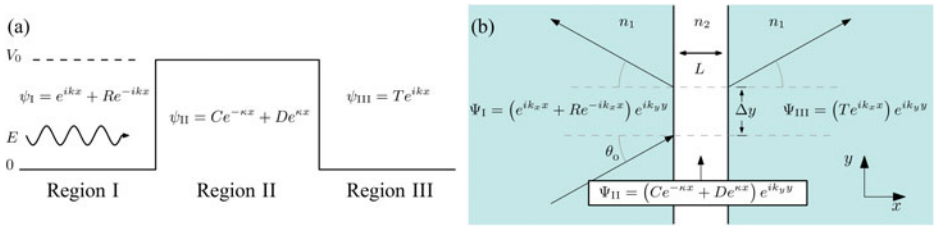

Figure 1. (a) Tunneling in quantum mechanics: a particle of energy E encounters a potential barrier of height V_0. (b) An optical analogue to (a): a photon undergoes frustrated total internal reflection.

direct measurements of this time delay as a function of barrier length are difficult to make, owing to the fine control required over the sub-wavelength air gap distance.

In this paper, we present a nematic-liquid-crystal-filled double-prism structure that can be used to simulate a quantum-mechanical barrier of variable height. The nematic liquid crystal's (LC) molecular director can be tuned with an externally-applied voltage to change the index contrast, and consequently the critical angle of the glass-LC interface. At oblique incidence this is equivalent to tuning the effective barrier height.

2. Time Delays in FTIR

Consider the double interface system shown schematically in Fig. 1(b). Light incident from a region of high refractive index encounters an interface with a material of lower index. If the light is incident above the critical angle, the Helmholtz equation admits the following stationary-state solutions: in region I, the incident and reflected plane waves Ψ_i and Ψ_r, respectively, in region III the transmitted wave Ψ_t, and in the barrier region the exponentially decaying solutions $\Psi_{(+)}$ and $\Psi_{(-)}$. Analytically, we can write

$$\Psi_{\mathrm{I}} = \Psi_i + \Psi_r = \left(e^{ik_x x} + Re^{-ik_x x}\right) e^{ik_y y}, \tag{1a}$$

$$\Psi_{\mathrm{II}} = \Psi_{(-)} + \Psi_{(+)} = \left(Ce^{-\kappa x} + De^{\kappa x}\right) e^{ik_y y}, \tag{1b}$$

$$\Psi_{\mathrm{III}} = \Psi_t = \left(Te^{ik_x x}\right) e^{ik_y y}, \tag{1c}$$

where the coefficients R, C, D, and T are deduced from the boundary conditions. An analogy can be made between the height of the barrier in Fig. 1(a) and the index contrast in Fig. 1(b) [4]:

$$\frac{E}{V_0} \leftrightarrow \frac{\cos^2\theta_0}{1-(n_2/n_1)^2}. \tag{2}$$

This analogy allows us to explore the intricacies of the quantum mechanical barrier tunneling phenomenon by measuring the optical time delay in FTIR as a function of the index of the barrier region.

There are several possible definitions of tunneling delay, and a thorough review would be outside the scope of this paper. We will therefore concentrate on the one most directly applicable to optical experiments. Most optical direct-time delay measurements are sensitive to the group delay τ_g, which represents the time-of-arrival of the peak of a gaussian pulse/wavefunction in the absence of severe distortion. This can be calculated in a

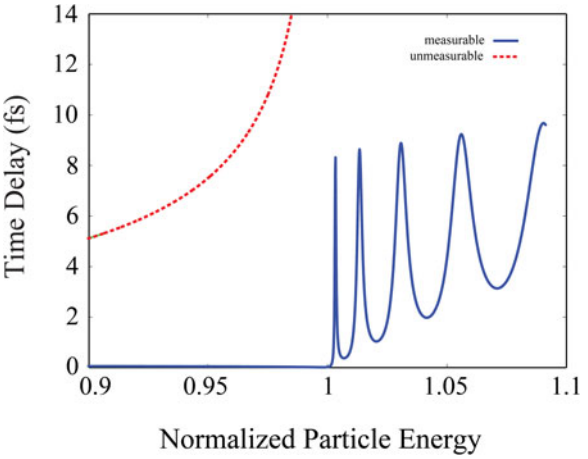

Figure 2. Measurable and unmeasurable parts of the total tunneling group delay plotted against the normalized particle energy $\cos^2\theta_0/(1 - n_2/n_1)^2$ for a photon undergoing FTIR for different values of n_2. In this simulation, $L = 8\ \mu$m, $\theta_0 = 63.5^\circ$, $\lambda = 727$ nm, $n_1 = 1.77$.

straightforward manner once the transmission coefficient T is known.

$$\tau_g = \left(\frac{\partial\varphi_0}{\partial\omega}\right)_{\theta_0} - \frac{\tan\theta_0}{\omega}\left(\frac{\partial\varphi_0}{\partial\theta_0}\right)_{\omega}, \qquad \varphi_0 = \arg T + k_x L. \tag{3}$$

The first term in this expression, $\partial\varphi_0/\partial\omega$, describes the delay contribution from the tunneling along the x-direction, while the second term gives the contribution to the total group delay that is due to the Goos-Hänchen shift Δy. For reasons explained in [4], in experimental implementations of FTIR the Goos-Hänchen contribution is identically compensated by a subsequent reduction in glass propagation length. We shall therefore refer to these two terms as the *measurable* and *unmeasurable* portions of the total group delay.

These quantities are plotted as a function of the normalized particle energy $\cos^2\theta_0/(1 - n_2/n_1)^2$ in Fig. 2. Two distinct regimes are observed. When $\cos^2\theta_0 > (1 - n_2/n_1)^2$ propagation in the barrier region is allowed and Fabry-Perot resonances are observed. In the tunneling regime, when $\cos^2\theta_0 < (1 - n_2/n_1)^2$, the Goos-Hänchen contribution dominates the total photonic delay and is orders of magnitude larger than the measurable portion. To observe this behavior experimentally, we have developed a liquid-crystal-filled double-prism structure where the index contrast can be tuned electronically.

3. Description of the Double-Prism Structure

The double-prism structure considered here is shown schematically in Fig. 3. A planar-aligned nematic liquid crystal cell with transparent indium-tin-oxide (ITO)-coated glass substrates is sandwiched between two equilateral glass prisms. To observe FTIR, a large index contrast between the liquid crystal layer and the substrates is required. For that reason, both the cell substrates and the prisms are made of high-index N-SF11 glass, which at $\lambda = 727$ nm has a refractive index of $n = 1.77$. A small amount of index-matching fluid ($n = 1.70$) is applied to the prism-cell interfaces to minimize unwanted reflections.

The LC cell preparation proceeds as follows: Two 3-mm thick N-SF11 substrates are sputter-coated with 30-nm layers of indium tin oxide (ITO) to serve as electrodes. Next, an

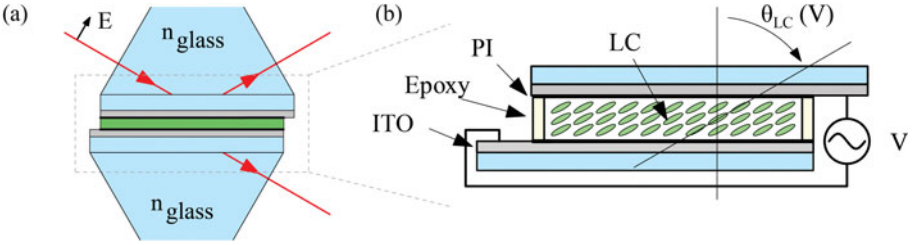

Figure 3. Diagram of the double-prism structure. In (a) a liquid crystal cell is sandwiched between two equilateral glass prisms. An exploded diagram of the liquid crystal cell is shown in (b). The substrates are coated with transparent Indium Tin Oxide (ITO) electrodes to facilitate electronic control of the liquid crystal molecular director rotation angle θ_{LC}, and thin polyimide layers (PI) to aid the alignment of the liquid crystal layer (LC).

approximately 15-nm alignment layer of polyimide is spin-coated on top of the ITO. The substrates are then subjected to a unidirectional mechanical buffing technique that shears the polyimide layer, causing the LC molecular director to preferentially align along the buffing direction when the cell is filled [6]. The cell is then constructed by placing spacers between the two processed faces: small amounts of 5-minute epoxy mixed with 5-μm glass beads are placed on the four corners of the cell, and pressure is applied while the epoxy mixture cures. The void thickness of cells prepared with this technique is typically in the range of 8–12 μm.

The cell is then filled with a uniaxial nematic LC mixture (E7: Merck) through capillary action. The edges of the cell are sealed with epoxy after filling to prevent evaporative loss and deterioration of the LC. Finally, wires are attached to the exposed ITO sections with conductive silver epoxy to allow for electronic control of the LC molecular director.

4. Simulation of Performance Under Realistic Conditions

To accurately simulate the performance of this device under realistic laboratory conditions, the rather simplistic model of section 2 must be extended to account for the anisotropy and disorder of the LC layer, and allow for a spread of input k-vectors. This can be accomplished by numerically solving Maxwell's equations in 4×4 matrix form for a multilayer slab structure [7]. Using this technique, the complex reflection and transmission coefficients are calculated as functions of the photon's frequency, its incidence angle, and the LC molecular director angle.

Figure 4 shows the calculated phase φ_R of the reflection coefficient as a function of the LC molecular director angle. In this simulation, the light is incident at $\theta_0 = 69.3^\circ$ from a glass region of refractive index $n_{\text{glass}} = 1.77$ onto an 8-μm-thick LC cell. The extraordinary and ordinary refractive indices used for the LC are $n_e = 1.63$ and $n_0 = 1.54$. These indices are a little lower and higher, respectively, than the expected values for E7 to correct for LC disorder. Since this method assumes plane wave incidence, we have convolved the phase with a Gaussian function to account for the spread of incidence angles present in our experiment (Fig. 4, solid line).

The expected optical time delay in reflection from this structure, $\partial\varphi_R/\partial\omega$, can be calculated as a function of applied voltage once the voltage dependence of the LC molecular director angle is known. This can be empirically determined from single-wavelength transmission measurements [8].

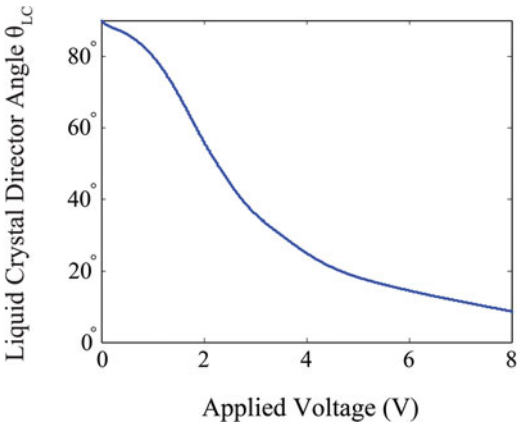

Figure 4. The predicted phase of the reflection coefficient based on the 4 × 4 matrix method described in the text for 727-nm light incident on an 8-μm liquid crystal cell. The parameters used are $\theta = 63.5^\circ$, $n_{\text{glass}} = 1.77$, $n_e = 1.63$ and $n_0 = 1.54$. The resulting phase is then convolved with a Gaussian function to account for a spread of input k-vectors (solid line).

The LC cell is placed between a polarizer and an analyzer and illuminated by a HeNe laser ($\lambda = 632.8$ nm) at normal incidence such that the input polarization is at 45° to the buffing direction. Transmission measurements are then taken as a function of applied voltage for both crossed and parallel analyzer configurations. The LC molecular director rotation angle can then be deduced from the ratio of the transmitted intensities.

The resulting behavior is shown in Fig. 5. In the absence of a driving field, the buffing process performed on the polyimide alignment layer causes the liquid crystal molecules to orient themselves along the direction of buffing, perpendicular to the surface normal ($\theta_{\text{LC}} = 90^\circ$). When an ac voltage is applied across the electrodes, it supplies a torque that twists the LC molecular director towards the surface normal.

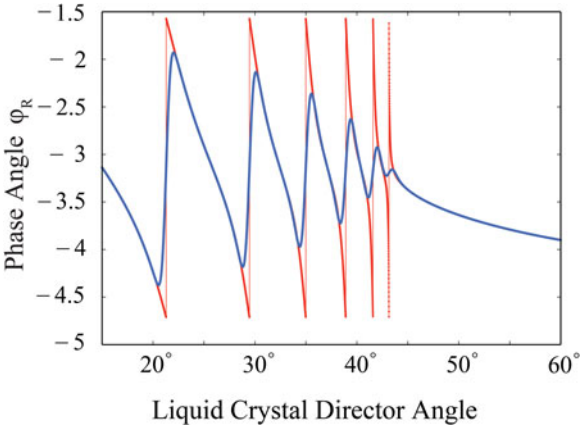

Figure 5. Dependence of the LC molecular director angle on applied voltage obtained from transmission measurements.

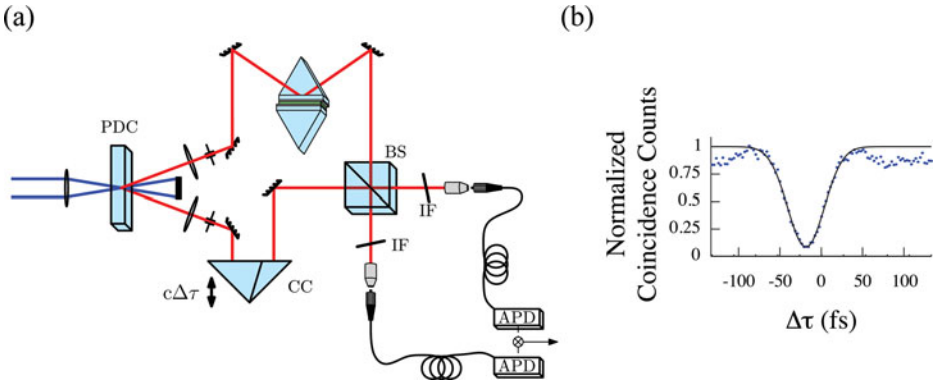

Figure 6. (a) Experimental setup for measuring reflection delay in FTIR with a Hong-Ou-Mandel interferometer. PDC is the parametric downconversion crystal for entangled photon generation, CC is a corner cube retroreflector on a motorized translation stage, BS is a non-polarizing 50/50 beamsplitter, IF are 10-nm bandpass interference filters centered at 727.6 nm, APD are avalanche photodiode single-photon counting modules. (b) Example data trace containing a Hong-Ou-Mandel dip, along with a numerical Gaussian fit.

5. Experiment

Optical time delays in reflection from this structure were measured with femtosecond precision using a Hong-Ou-Mandel interferometer [9, 10]. In our experimental setup (Fig. 6) entangled pairs of linearly-polarized photons are generated through type I spontaneous parametric downconversion in a 3-mm thick BBO crystal that is pumped by a 1-W continuous-wave argon-ion laser ($\lambda = 363.8$ nm). Interference filters set the photon's bandwidth to be 10 nm, centered around 727.6 nm. One photon is sent through a path of known length while the other is sent to a test arm that contains the double-prism structure. The photons are then recombined in a 50–50 beam splitter whose output ports are monitored by

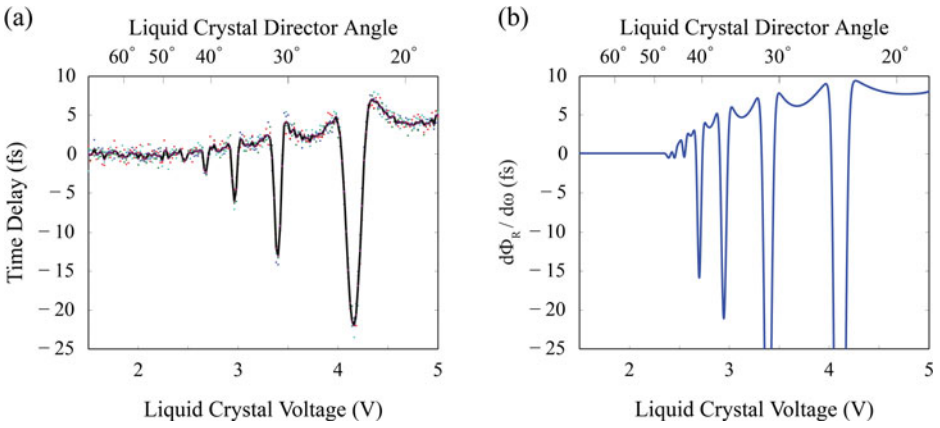

Figure 7. (a) Reflection delay in FTIR from the double-prism structure. The black line is the arithmetic mean of four individual data sets. Each data point represents an individual Hong-Ou-Mandel trace with 102 seconds of integration time. (b) Predicted $d\Phi_R/d\omega$ for 727-nm light propagating through an 8-μm liquid crystal cell.

avalanche photodiodes in coincidence while the length of the known arm is varied. When the interferometer is balanced, both photons exit from the same port and the coincidence count rate is reduced. The position of complete destructive interference can be determined with sub-fs resolution, though in practice the resolution may be limited by thermal drifts or other sources of noise. This procedure is repeated for different applied voltages, and the shift of the Hong-Ou-Mandel dip relative to $V = 0$ is used to extract the time delay. Further details about the experimental procedure are given in [11].

The experimentally measured reflection time delays are shown in Fig. 7, along with a plot of the expected group delay calculated numerically. The experimental data are in excellent agreement with the model predictions. As before, two distinct regimes are observed. For voltages above approximately 2.2 V, Fabry-Perot resonances are observed. Note that the sharp dips on resonance arise from the interference from the Gaussian beam k-vector distribution. The delay in the tunneling region appears to be identically zero within the experimental uncertainty, confirming that the Goos-Hänchen contribution is suppressed in this type of measurement.

6. Conclusions

In this paper, we have presented a double-prism structure under frustrated-total-internal reflection conditions that, with the aid of an electrically-tunable nematic liquid crystal cell effectively simulates a quantum-mechanical barrier of variable height. In contrast to mechanically-tuned double-prism systems, in which the deleterious effects of stress-induced birefringence must be taken into account, our structure has no moving parts and introduces no significant beam deviations during the tunneling process. This has enabled us to experimentally measure the time delay experienced by single photons upon frustrated total internal reflection with sub-fs precision.

These results strongly support a cavity interpretation of the tunneling process. Moreover, our experiments confirm our earlier prediction that the Goos-Hänchen contribution is suppressed in the measurable portion of tunneling delay in this geometry [4], which may prove important for the fabrication of optical analogs to the tunnel junction and other photonic devices [12–14].

Acknowledgments

We acknowledge the assistance of Kenneth Marshall and Simon Wei in constructing the LC cell. S. G. L. is supported by the NSF (Grant No. DUE-0920500). This work was supported by the US Defense Threat Reduction Agency–Joint Science and Technology Office for Chemical and Biological Defense (Grant No. HDTRA1-10-1-0025) and by the Canada Excellence Research Chairs Program.

References

[1] Wigner, E. P. (1955). *Phys. Rev.*, *98*(1), 145–147.
[2] Winful, H. G. (2006). *Phys. Rep.*, *436*, 1–69.
[3] Winful, H. G., & Zhang, C. (2009). *Phys. Rev. A*, *79*(2), 023826.
[4] Gehring, G. M., Liapis, A. C., & Boyd, R. W. (2012). *Phys. Rev. A*, *85*(3), 032122.
[5] Papoular, D. J., Clade, P., Polyakov, S. V., Migdall, A., Lett, P. D., & Phillips, W. D. (2008). *Opt. Express*, *16*, 16005–16012.
[6] Geary, J. M., Goodby, J. W., Kmetz, A. R., & Patel, J. S. (1987). *J. Appl. Phys.*, *62*(10), 4100–4108.

[7] Berreman, D. W. (1972). *J. Opt. Soc. Am.*, *62*(4), 502–510.
[8] Wu, S.-T., Efron, U., & Hess, L. D. (1984). *Appl. Opt.*, *23*, 3911–3915.
[9] Hong, C. K., Ou, Z. Y., & Mandel, L. (1987). *Phys. Rev. Lett.*, *59*, 2044–2046.
[10] Steinberg, A. M., Kwiat, P. G., & Chiao, R. Y. (1993). *Phys. Rev. Lett.*, *71*, 708–711.
[11] Gehring, G. M., Liapis, A. C., Lukishova, S. G., & Boyd, R. W. (2013). *Phys. Rev. Lett.*, *111*(3), 030404.
[12] Lukishova, S. G., Pashinin, P. P., Batygov, S. K., Arkhangelskaya, V. A., Poletimov, A. E., Scheulin, A. S., & Terentiev, B. M. (1990). *Laser Part. Beams*, *8*(1–2), 349–360.
[13] Jian A. Q., & Zhang, X. M. (2013). *IEEE J. Sel. Top. Quantum Electron.*, *19*(3), 9000310.
[14] Sun, D. G. (2013). *J. Appl. Phys.*, *114*, 104502.